

Characterization and deactivation of sulfided red mud used as hydrogenation catalyst

Jorge Alvarez, Roberto Rosal, Herminio Sastre, Fernando V. Díez *

Department of Chemical Engineering, University of Oviedo 33071-Oviedo, Spain

Received 26 January 1995; revised 29 March 1995; accepted 29 March 1995

Abstract

Red mud is a residue in the production of alumina by the Bayer process. It contains oxides of iron and titanium, and has been shown to be active in sulfided form as hydrogenation catalyst. The evolution of sulfided red mud activity and selectivity with reaction time was studied for the hydrogenation of a light fraction of an anthracene oil. Texture, morphology and composition of fresh red mud, and catalyst samples collected at different reaction times, were characterized by nitrogen adsorption, SEM and SEM-EDX. It was found that the catalyst loses surface area and superficial iron as the reaction proceeds. The decrease of catalytic activity can be explained by a combination of both phenomena.

Keywords: Red mud; Deactivation; Hydrogenation; Scanning electron microscopy

1. Introduction

Red mud is a material containing mainly oxides of iron, aluminium, titanium, silicon, calcium and sodium, and is produced as a residue in the manufacture of alumina by the Bayer process. Sulfided red mud was found to be active as a hydrogenation catalyst as early as 1950 [1]. Further studies showed the catalytic activity of sulfided red mud for the liquefaction of coal [2–4], biomass [5], and for the hydrogenation of pure organic compounds such as naphthalene, phenanthrene and pyrene [4,6].

In a previous work [7], sulfided red mud was tested as a catalyst for the hydrogenation of anthracene oil, a fraction obtained by distillation of coal tar, containing two- to four-rings condensed aromatic hydrocarbons. These compounds can transform into hydroaromatics by catalytic hydrogenation, yielding a hydrogenated

* Corresponding author. E-mail vega@dwarf1.quimica.uniovi.es, tel. (+34-8) 5103508, fax. (+34-8) 5103434.

solvent with high hydrogen-donor capacity. Hydrogenated anthracene oil can be used in processes such as coal liquefaction [8,9], oil–coal coprocessing [10], and coke production by carbonization of low-rank coals with pitch-like materials [11].

In the aforementioned work [7], it was found that, although to a lesser degree than if commercial catalysts such as Ni/Mo on γ -alumina are used, anthracene oil hydrogenated in the presence of sulfided red mud contained appreciable concentrations of hydroaromatics, especially dihydroanthracene, dihydrophenanthrene and tetrahydrofluoranthene, that are reported [12,13] to be among the most active hydrogen donors. Hydrogenation reactions were carried out in a bench-scale continuous trickle bed at 623 K, 10 MPa, and constant catalytic activity.

In order to evaluate the practical usefulness of a catalyst, it is very important to determine the time on stream after which the catalytic activity falls to an unacceptable level. In this work, the evolution with time of the activity and selectivity of red mud used as a catalyst for the hydrogenation of anthracene oil was studied. Reactions were carried out at constant temperature, pressure and flow-rates. Catalyst samples were collected after different reaction times and characterized by BET nitrogen adsorption, scanning electron microscopy (SEM), and scanning electron microscopy–energy-dispersive X-ray (SEM-EDX).

2. Experimental

2.1. Materials

Red mud, as a residue of the caustic digestion of bauxite, contains all the elements present in bauxite that are insoluble or partially soluble in caustic soda, concentrated about five times, plus sodium and calcium coming from the reagents added during the digestion process. Mineralogically, the main constituents of red mud are hematites, rutile, goethite, sodalite, boehmite and gibbsite. The red mud used in this work was supplied by the San Ciprián (La Coruña, Spain) plant of the Spanish aluminium company Inespal. The main constituents of the red mud were analyzed by atomic absorption spectrometry and volumetric methods after acid dissolution and alkaline fusion. Details of the analytical method are given elsewhere [14], while the composition of the red mud can be found in Table 1.

Sulfided red mud catalytic activity was tested by hydrogenating a light fraction of anthracene oil supplied by Nalon-Chem (Asturias, Spain), with the composition given in Table 2.

2.2. Catalyst characterization

Catalyst pore structure and surface area was measured by nitrogen adsorption with a Micromeritics Asap 2000 apparatus.

Table 1
Bulk and EDX composition of red mud

Element	Bulk composition (wt.-%)	EDX composition (wt.-%)
Fe	19.7	21.7
Ti	13.0	11.9
Al	7.9	7.4
Na	3.7	3.0
Ca	5.1	4.9
Si	4.7	3.6
P	not measured	0.7
V	not measured	0.3
Cl	not measured	0.3

Catalyst morphology was studied by SEM in a JSM-6100 apparatus, the catalyst samples being previously gold-coated. The SEM apparatus is equipped with a Link X-ray microanalyzer that provides a quantitative chemical analysis of a catalyst surface layer to a depth of about 1 μm , and supplies information on the distribution of certain elements, providing maps in which the brightness of every pixel depends on the concentration of this element. For this kind of analysis, catalyst samples must be polished and carbon coated.

2.3. Reaction studies

The hydrogenation experiments were carried out in a continuous trickle bed reactor with a 9 mm internal diameter, 45 cm long stainless steel cylinder. 2.0 g of red mud were placed in the central section of the reactor, the upper and lower sections being filled with 0.25–0.08 mm particles of low-area inert alumina. Red

Table 2
Composition of anthracene oil (wt.-%)

Naphthalene	4.0
Acenaphthene	5.9
Dibenzofuran	3.1
Fluorene	4.9
9,10-Dihydroanthracene	0.8
Phenanthrene	18.2
Anthracene	4.4
Carbazole	2.9
Fluoranthene	10.2
Pyrene	6.2
2-Methylnaphthalene	1.0
Dibenzothiophene	1.2
Methylantracene	1.1
Methylphenanthrene	1.2
Methylpyrene	1.5
Chrysene	1.7
Triphenylene	1.8

mud was sulfided in situ before use by passing a mixture of 10% hydrogen sulfide in hydrogen at atmospheric pressure through the reactor, heated to 673 K, for 4 h. The liquid feed, consisting of 20 wt.-% anthracene oil dissolved in toluene, for easier handling, flowed downwards through the reactor, concurrently with hydrogen. 1 wt.-% carbon sulphide was added to the liquid feed to maintain the catalyst in the sulfided form. Reaction products were collected in a cylindrical receiver, and liquid samples were withdrawn by emptying the receiver at different time intervals. Hydrogenated anthracene oil was analyzed by gas chromatography using a capillary fused silica column with apolar stationary phase SE-30. Peak assignment was performed by gas chromatography–mass spectrometry.

All the experiments were carried out under the same reaction conditions: pressure 10 MPa, temperature 623 K, hydrogen flow-rate $4 \cdot 10^{-6} \text{ N m}^3/\text{s}$, and liquid flow-rate (at room conditions) 0.6 ml/min. Further details of the reaction experimental set up and procedure are given in ref. [7].

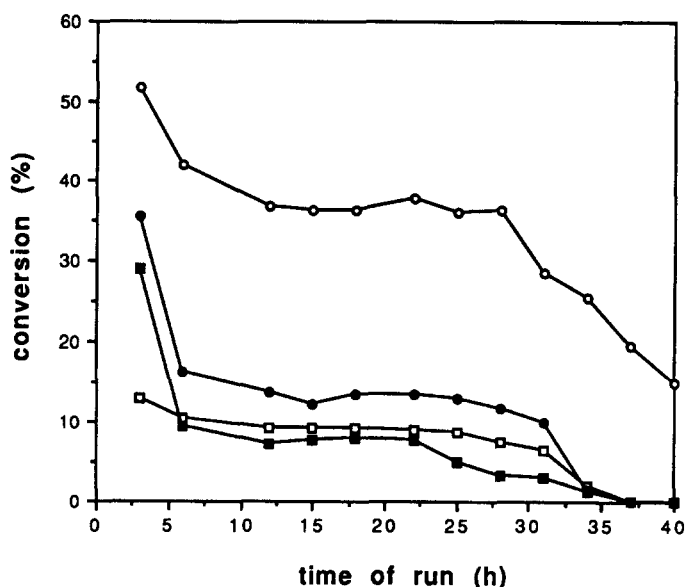


Fig. 1. Evolution of conversions with run time for: (○) anthracene, (□) phenanthrene, (■) fluoranthene, (●) pyrene.

Table 3
Textural characteristics of different red mud samples, obtained by nitrogen adsorption

	Fresh		After reaction time:		
	Unsulfided	Sulfided	3 h	12 h	40 h
BET specific surface (m^2/g)	24.3	29.5	27.9	18.3	16.2
BJH desorption pore volume (cm^3/g)	0.086	0.090	0.067	0.045	0.034
BET average pore diameter (nm)	12.1	10.5	10.6	10.0	8.9

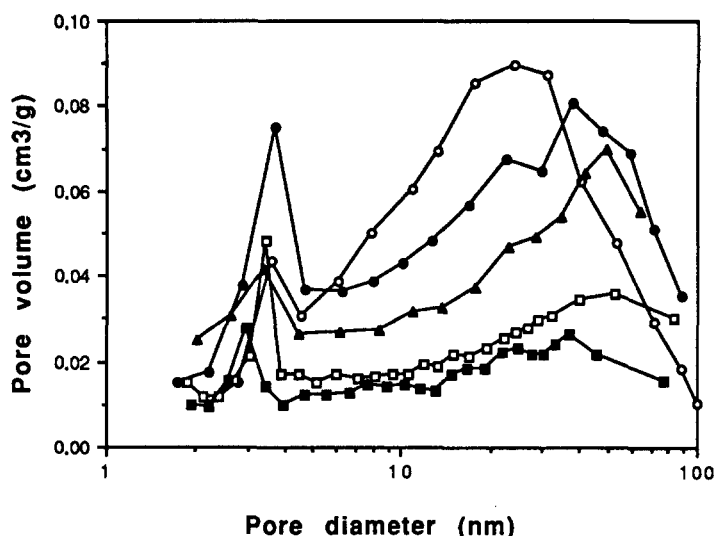


Fig. 2. Pore volume distributions of the red mud: (○) fresh, unsulfided; (●) fresh, sulfided; (▲) after 3 h; (□) after 12 h; (■) after 40 h.

3. Results and discussion

The anthracene oil constituents that were hydrogenated to a measurable degree at reaction conditions were: anthracene, phenanthrene, fluoranthene, and pyrene, yielding as hydrogenated products 9,10-dihydroanthracene, 9,10-dihydrophenanthrene, 1,2,3,10b-tetrahydrofluoranthene and 4,5-dihdropyrene, respectively. It has been shown [15] that hydrogenation of those compounds accounts for more than 75% of the total hydrogen consumption. Fig. 1 shows the evolution of the conversion of the different compounds with reaction time. The evolution of the catalyst activity followed the usual path of an initial period of fast activity decay, followed, after 6 h approximately, by a period of about 25 h of slowly declining activity. After about 38 h of run, the activity quickly decreased to a point at which the only reactant converted was anthracene. Although the profile of the evolution of conversion with time was similar for all the reactants, there are some differences: phenanthrene showed a less sharp decline of conversion in the initial deactivation period, and anthracene showed not only a higher conversion, but also a slower decrease of conversion during the full time of reaction. If the average conversion is taken as:

$$\text{average conversion} = \frac{\sum \text{compounds in feed} - \sum \text{compounds in product}}{\sum \text{compounds in feed}}$$

where \sum compounds is the sum of the concentrations of anthracene, phenanthrene, fluoranthene and pyrene, the average conversion of 0.254 measured after 3 h, decreased to 0.123 after 12 h and to 0.018 after 40 h.

Catalyst samples were collected after 3 h, and 12 h reaction time, corresponding to the catalyst in the period of declining activity, and 40 h, corresponding to the

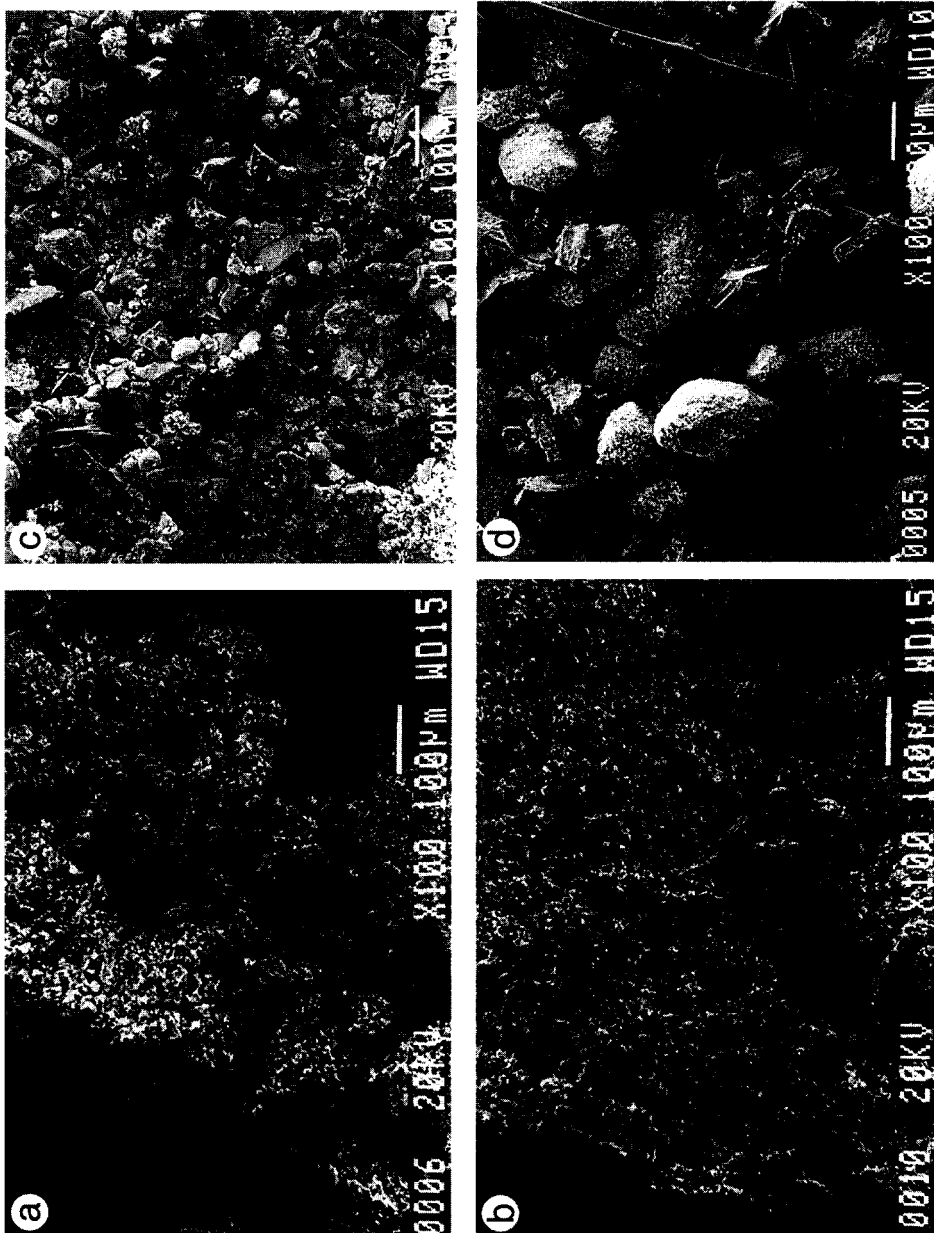


Fig. 3. SEM photographs of the surface of red mud: (a) fresh, unsulfided; (b) fresh, sulfided; (c) after 12 h run time; (d) after 40 h run time.

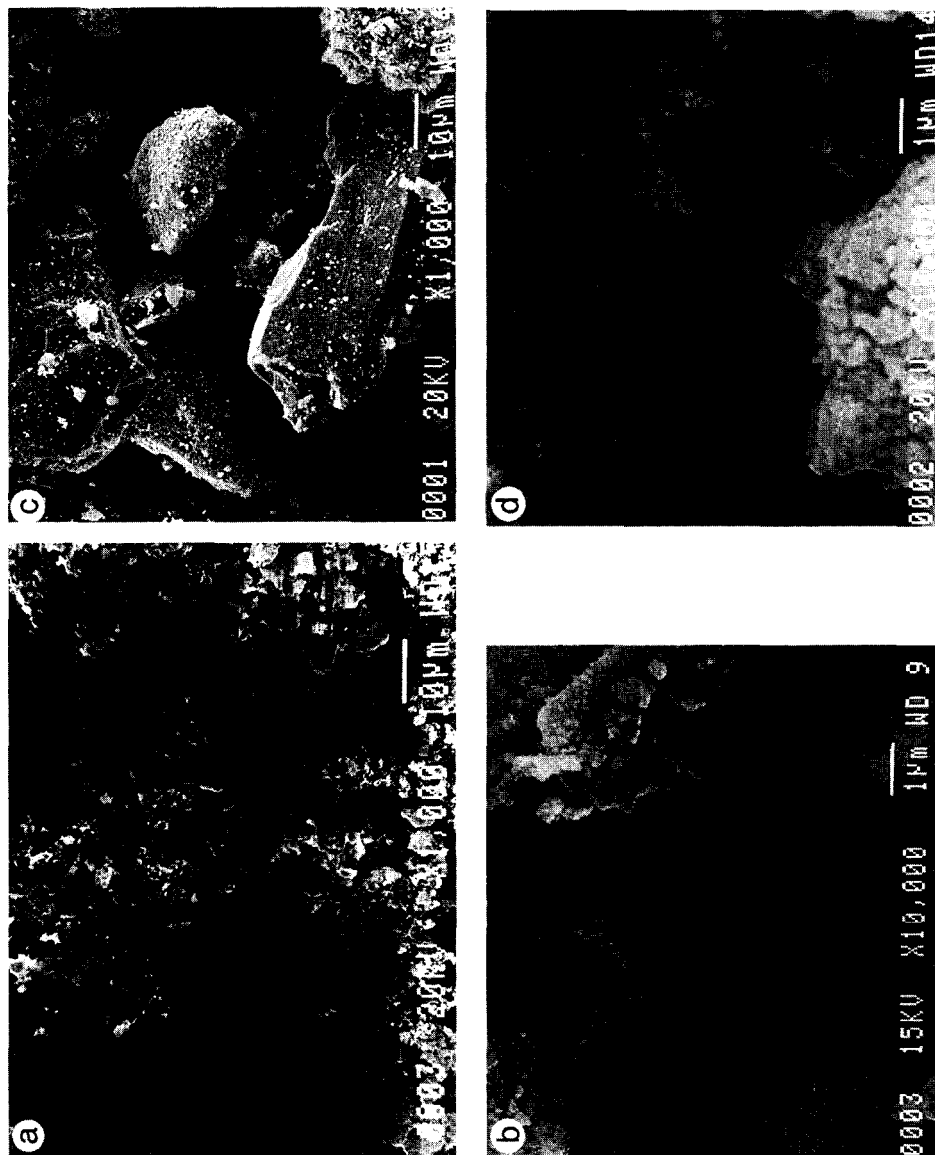


Fig. 4. SEM photographs of the surface of red mud: (a) fresh, sulfided; (b) fresh, sulfided; (c) after 12 h run time; (d) after 12 h run time.

Table 4
EDX composition of sulfided red mud after different reaction times in the presence of H₂S (wt.-%)

Element	Reaction time			
	0 h	3 h	12 h	40 h
Fe	36.7	36.2	35.8	33.7
Ti	17.9	13.8	13.4	14.2
S	14.5	14.5	19.4	20.1
Al	11.3	12.1	14.9	16.0
Ca	7.6	5.1	5.1	5.1
Si	6.2	6.6	4.1	3.5
Na	4.0	2.4	2.4	2.2
Cl	1.0	1.0	3.7	4.0
P	0.8	0.6	1.0	0.7
V	0.3	0.4	0.4	0.3

catalyst being almost completely deactivated. These samples, and samples of fresh unsulfided and sulfided catalyst, were characterized by nitrogen adsorption and SEM.

The results of textural characterization by nitrogen adsorption of the catalyst samples are given in Table 3 and Fig. 2. Sulfidation slightly increased the red mud surface area and decreased the average pore diameter. The run strongly affected the surface area and pore volume: after 12 h reaction time, the surface area decreased to 62%, and pore volume to 50%. During the next 28 h, catalyst pore volume and surface area continued decreasing, but less markedly.

Fig. 3 and Fig. 4 present SEM photographs of the red mud in different conditions. In Fig. 3 the change of the catalyst morphology as the reaction proceeded can be observed: the granulated, uniform surface of fresh unsulfided and sulfided red mud was transformed in a non-uniform surface formed by particles of increasing size. At higher magnifications (Fig. 4), it can be observed that fresh red mud is made up of particles partially covered by small granules. After 12 h run, besides zones similar in appearance to the fresh red mud (Fig. 4a), other zones appeared formed by larger, flat-surfaced particles, which were less covered by granules than fresh red mud (Fig. 4c and d).

Table 4 gives the concentration of the different red mud samples measured by SEM-EDX. As the reaction proceeded, iron decreased slightly, while titanium, calcium, silicon and sodium decreased more markedly. The elements that increased their composition were sulfur and aluminium, and especially chlorine.

Maps of the elements in the catalyst samples obtained by EDX are shown in Figs. 5–9. In these maps, the brightness of every pixel is related to the intensity of emission of the characteristic K α line of each element. White corresponds to a high concentration of a given element, and black to the absence of this element, while greys correspond to intermediate concentrations. The pictures were obtained by setting two different levels of brightness, for the elements in high concentration

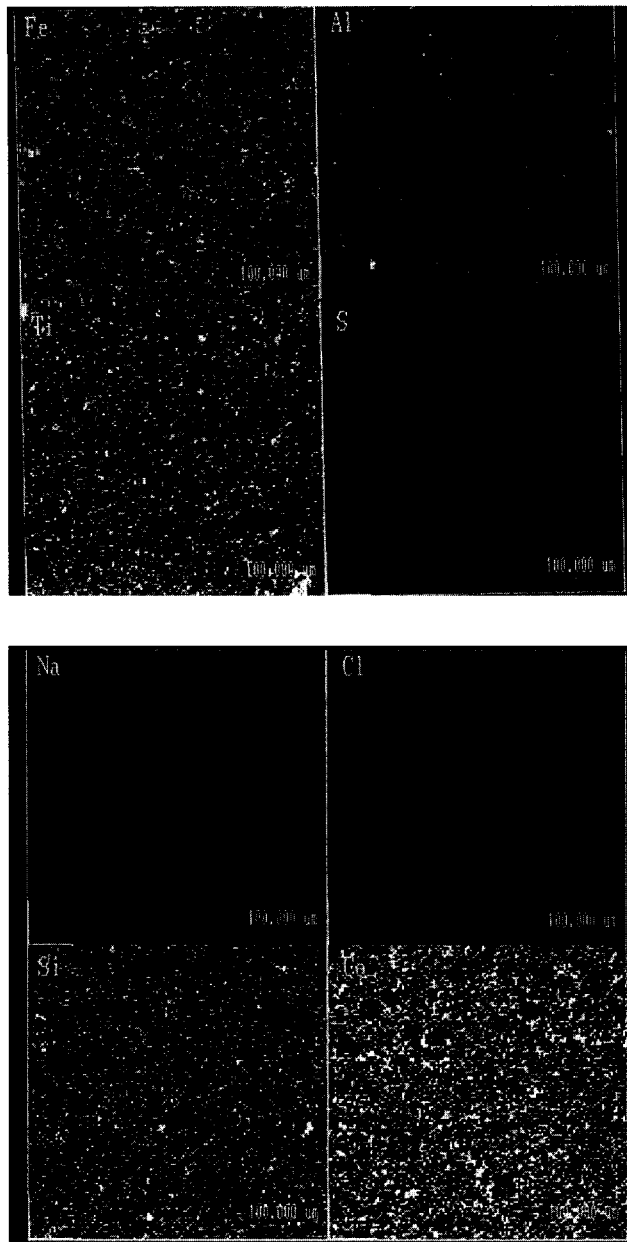


Fig. 5. SEM-EDX maps of distribution of elements: fresh, unsulfided red mud.

(iron, aluminium, titanium and sulfur), and in low concentration (sodium, chlorine, silicon and calcium). Fig. 5, corresponding to fresh, unsulfided red mud, shows the elements distributed uniformly on the surface. Sulfur and chlorine are present in very small amounts. After sulfidation (Fig. 6), the superficial concentration of aluminium and sulfur increased, aluminium being concentrated in a part of the surface, in which iron is absent. Titanium, sulfur, silicon and calcium were asso-

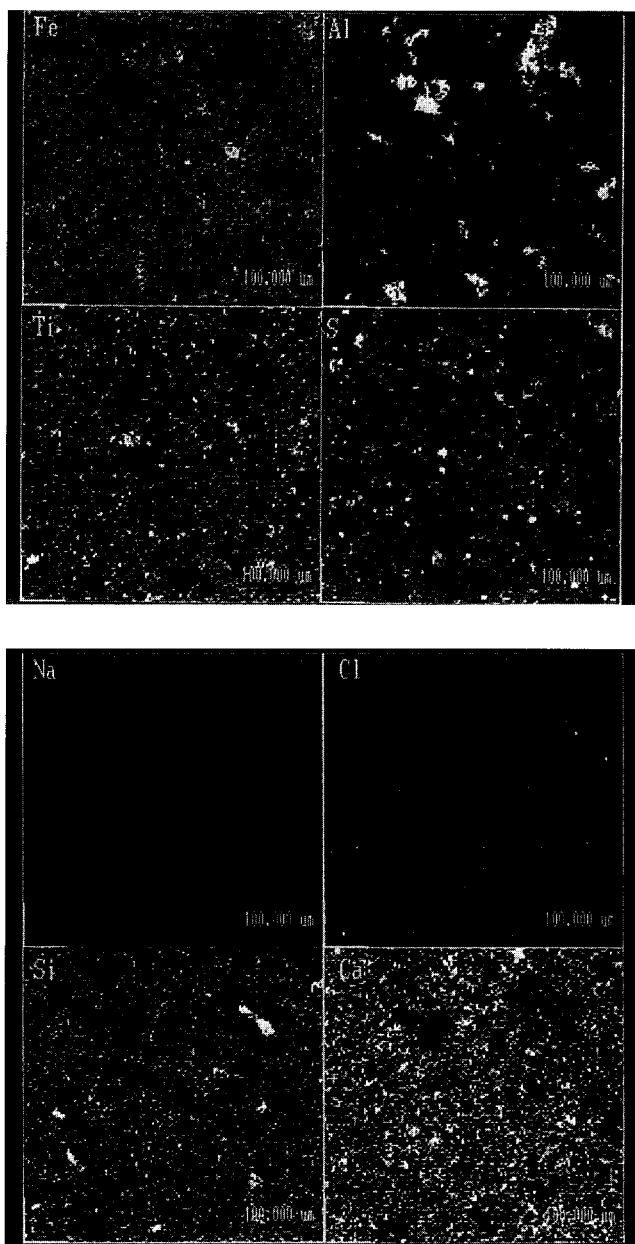


Fig. 6. SEM-EDX maps of distribution of elements: fresh, sulfided red mud.

ciated with iron. After 12 h reaction time, aluminium occupied most of the surface, the rest being covered by iron and associated elements (titanium, sulfur, silicon and calcium). The presence of chlorine in the surface increased considerably, and was also associated with iron. A small amount of sodium appeared, associated with iron and chlorine. The same tendency of aluminium to occupy progressively the catalyst surface, and the decreasing presence of iron, was observed after 40 h reaction time (Fig. 9).

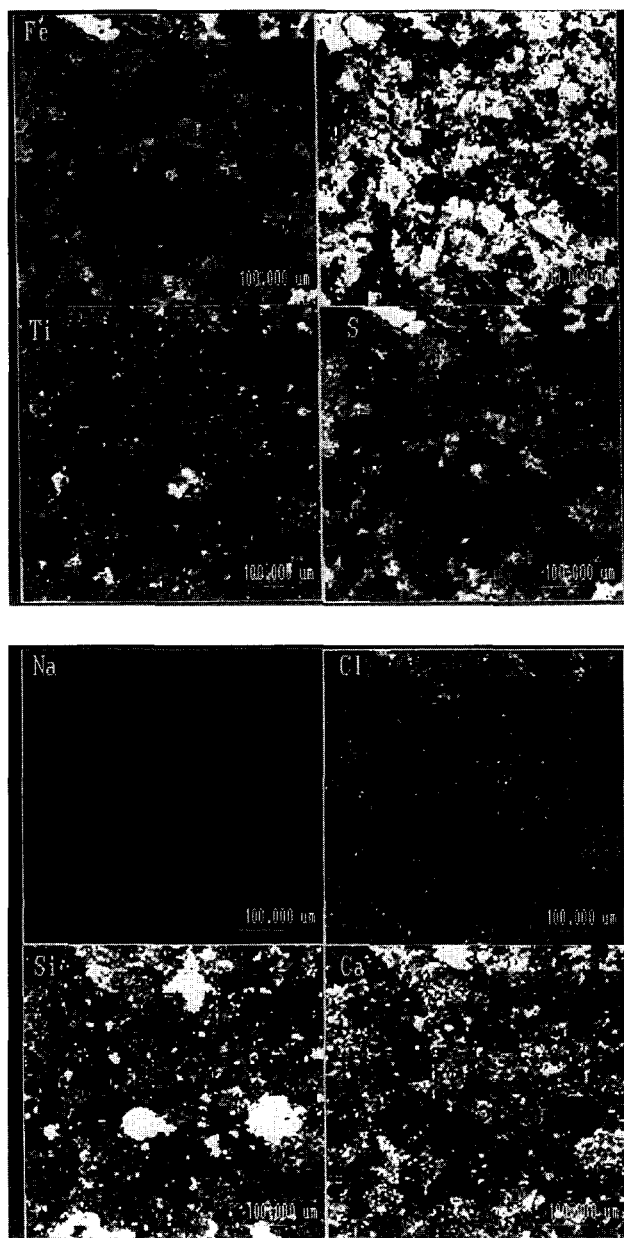


Fig. 7. SEM-EDX maps of distribution of elements: red mud after 3 h run time.

The brightness of every pixel of the EDX maps, B , can be quantified on a scale of 0 (black) to 1 (maximum degree of brightness). Fig. 10 shows the cumulative brightness distributions (fraction of the sample surface that has a brightness less than a given level B) for the iron maps of the different catalyst samples. From this figure, it can be observed that the surface with little presence of iron (relative brightness less than 0.1) increased slightly after sulfiding (from 10.4% total surface

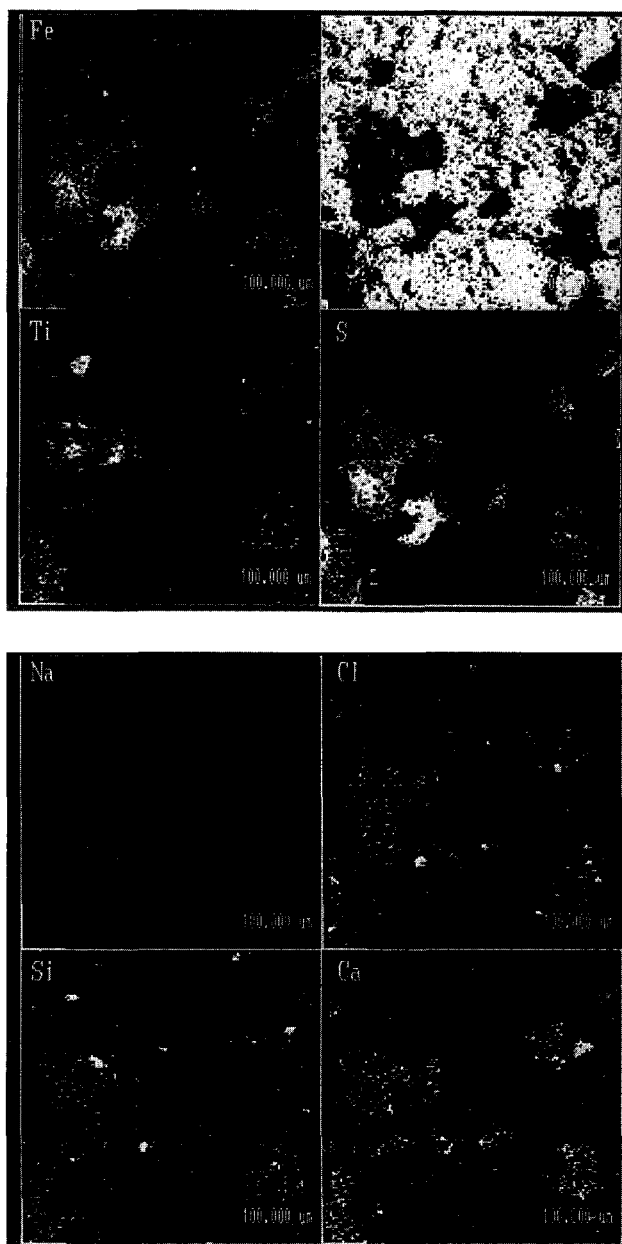


Fig. 8. SEM-EDX maps of distribution of elements: red mud after 12 h run time.

to 15.1%), and very markedly after 12 h reaction time (57.1%), reaching 77.2% after 40 h reaction time. $\sum B_i S_i$ (S_i being the surface fraction corresponding to a brightness B_i) can be taken as an alternative measure of iron content in the 1 μm surface layer. If iron content for fresh unsulfided red mud measured in this way is taken as a reference, the relative iron content for fresh sulfided red mud was 0.94, after 3 h reaction time 0.90, after 12 h reaction time 0.66, and after 40 h, 0.26. The

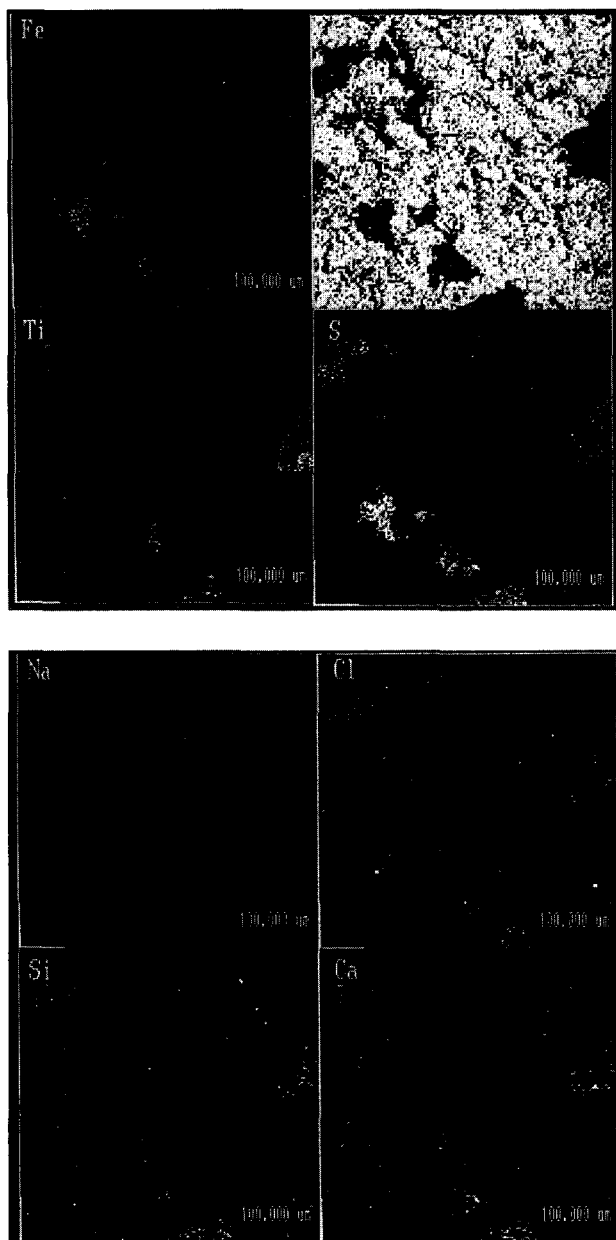


Fig. 9. SEM-EDX maps of distribution of elements: red mud after 40 h run time.

decrease of iron quantified by this method was much more marked than that given by the SEM-EDX data of Table 4.

Average conversion, as defined previously, shows an almost linear relationship with the relative catalyst iron content in the $1 \mu\text{m}$ surface layer, defined as the product of the surface area and iron content measured from the EDX maps. The decrease in iron, assumed to be the active phase as iron sulfide, fully explains the deactivation observed during the reaction run.

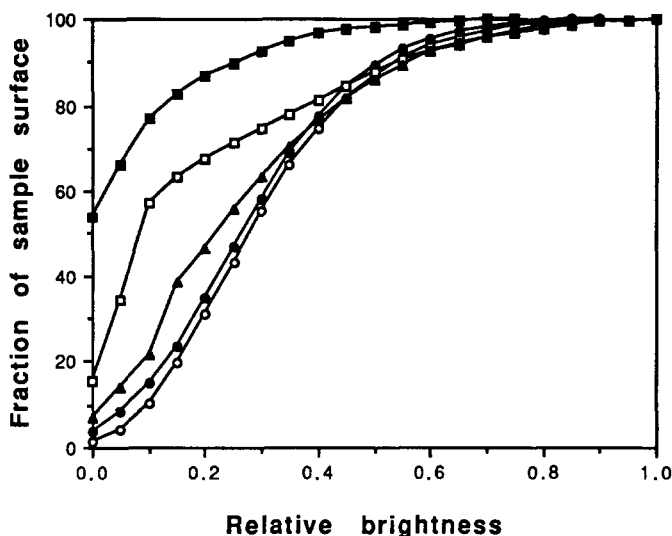


Fig. 10. Cumulative brightness distributions for the Fe EDX maps of the red mud: (○) fresh, unsulfided; (●) fresh, sulfided; (▲) after 3 h; (□) after 12 h; (■) after 40 h.

It was not possible to compare SEM photographs with EDX maps directly, as they are obtained from different catalyst samples prepared by different treatments. Nevertheless, observing SEM photographs of Fig. 3 and Fig. 4, and EDX maps of Figs. 5–9, one can speculate that iron and titanium corresponded to small granules, homogeneously distributed on the surface of fresh red mud, while the surface of the larger flat-surfaced particles present in aged red mud, would mainly consist of alumina. On the surface of the aged catalyst, iron would be present as small granules deposited non-uniformly on the larger particles.

Acknowledgements

This work was supported by the Spanish Interministerial Commission for Science and Technology under Grant MAT92-0807. The authors are grateful to Mr. Alfredo Quintana, of the Electron Microscopy Service of the University of Oviedo.

References

- [1] S. Weller, M.G. Pelipetz, S. Friedman and H.H. Storch, *Ind. Eng. Chem.*, 42 (1950) 330.
- [2] D. Garg and E.N. Givens, *Ind. Eng. Chem. Process Des. Dev.*, 24 (1985) 66.
- [3] S. Sato, M. Morita, T. Hashimoto, I. Mitunori, K. Chiba and H. Tagaya, *Fuel*, 68 (1989) 622.
- [4] A. Eamsiri, R. Jackson, K.C. Pratt, V. Christov and M. Marshall, *Fuel*, 71 (1992) 449.
- [5] B. Klopties, W. Hodek and F. Bandermann, *Fuel*, 69 (1990) 448.
- [6] K.C. Pratt and V. Christoverson, *Fuel*, 61 (1982) 460.
- [7] J.J. Llano, R. Rosal, H. Sastre and F.V. Díez, *Fuel*, 73 (1994) 688.
- [8] D.D. Whitehurst, T.O. Mitchell and M. Farcasiu, *Coal Liquefaction*, Academic Press, New York, 1980.

- [9] K. Chiba, H. Tagoya, T. Kobayashi and Y. Shibuya, *Ind. Eng. Chem. Res.*, 26 (1987) 1329.
- [10] S.E. Moschopedis, J.G. Hawkins, J.F. Fryer and J.G. Speight, *Fuel*, 59 (1980) 647.
- [11] T. Yotono and H. Marsh, in H.D. Schultz (Editor), *Coal Liquefaction Products: NMR Spectroscopic Characterization and Production Processes*, Wiley, New York, 1983, p. 125.
- [12] I. Mochida, O. Kazumasa and Y. Korai, *Fuel*, 64 (1985) 906.
- [13] C.E. Snape, F.J. Derbyshire, H.P. Kottenste and N.W. Smith, *Am. Chem. Soc. Div. Fuel Chem. Prep.*, 34 (1989) 793.
- [14] J.J. Alvarez Rodríguez, M.Sc. Dissertation, University of Oviedo, 1994.
- [15] R. Rosal, F.V. Díez and H. Sastre, *Fuel*, 71 (1992) 761.